J. Membrane Biol. 188, 55–71 (2002)
DOI: 10.1007/s00232-001-0174-2

The Journal of
Membrane
Biology

CFTR is a Monomer: Biochemical and Functional Evidence

J.-H. Chen, X.-B. Chang, A.A. Aleksandrov, J.R. Riordan
Mayo Foundation and Mayo Clinic Scottsdale, S. C. Johnson Medical Research Center, 13400 E. Shea Blvd., Scottsdale, AZ 85259, USA

Received: 28 December 2001/Revised: 18 March 2002

Abstract. Although the CFTR protein alone is sufficient to generate a regulated chloride channel, it is unknown how many of the polypeptides form the channel. Using biochemical and functional assays, we demonstrate that the CFTR polypeptide is a monomer. CFTR sediments as a monomer in a linear, continuous sucrose gradient. Cells co-expressing different epitope-tagged CFTR provide no evidence of co-assembly in immunoprecipitation and nickel affinity binding experiments. Co-expressed wild-type and ΔF508 CFTR are without influence on each other in their ability to progress through the secretory pathway, suggesting they do not associate in the endoplasmic reticulum. No hybrid conducting single channels are seen in planar lipid bilayers with which membrane vesicles from cells co-expressing similar amounts of two different CFTR conduction species have been fused.

Key words: ABC protein — CFTR — Chloride channel — Cystic fibrosis — Quaternary structure — CFTR monomer

Introduction

Adenine nucleotide binding cassette (ABC) proteins are products of a very large gene family, primarily membrane proteins that mediate translocation of solutes across lipid bilayers (Higgins, 1992). Each of these transporter units contains two membrane-integrated domains and two nucleotide-binding domains either in a single polypeptide or two or four associating polypeptides (Doige & Ames, 1993; Higgins, 1992; Dean, Rzhetsky & Allikmets, 2001). In the cases of the single large polypeptides their active oligomeric structures have generally not yet been determined. The P-glycoprotein multidrug transporter has been most studied from this perspective (Boscoboinik et al., 1990; Naito & Tsuruo, 1992; Poruchynsky & Ling, 1994; Loo & Clarke, 1996; Jette, Potier & Beliveau, 1997; Juvvadi et al., 1997; Rosenberg et al., 1997; Taylor et al., 2001). Although there is some evidence that it may form dimers (Boscoboinik et al., 1990; Naito & Tsuruo, 1992; Poruchynsky & Ling, 1994; Jette et al., 1997; Juvvadi et al., 1997) several recent studies, including low-resolution 3-D structure, indicate that it exists and functions as a monomer (Loo & Clarke, 1996; Rosenberg et al., 1997; Taylor et al., 2001). The only convincing example of an oligomeric functional ABC protein is the SUR1 subunit within the K_{ATP} channel (Aguilar-Bryan et al., 1998). This channel is constituted by four Kir6.2 inwardly rectifying potassium channel polypeptides, each associated with one SUR1, resulting in an octamer (Clement et al., 1997; Inagaki, Gonoi & Seino, 1997; Shyng & Nichols, 1997). However, this assembly essentially reflects the typical tetrameric structure of potassium channels (MacKinnon, 1991; Liman, Tytgat & Hess, 1992; Yang, Jan & Jan, 1995; Corey et al., 1998); there is no evidence of interactions between the four SUR1 subunits.

The CFTR polypeptide alone without additional proteins is sufficient to generate a regulated low-conductance chloride channel (Bear et al., 1992; Ramjeesingh et al., 1997). However, it is unknown how many CFTR polypeptides constitute the channel. As briefly outlined above, the bias from the ABC protein perspective might point in the direction of a monomer. In contrast, since nearly all known ion channels are homo- or hetero-oligomers (Hille, 2001), the possibility that CFTR may possess a quaternary structure also has to be considered.

In an initial assessment of whether CFTR polypeptides self-associate, Marshall et al. (1994) co-expressed full-length and C-terminally-truncated forms

Correspondence to: J.R. Riordan; email: riordan@mayo.edu

of CFTR and immunoprecipitated with an antibody that recognized an epitope at the extreme C-terminus and hence absent from the truncated species. The latter was not co-immunoprecipitated with the full-length protein, implying that self-association did not occur or was not maintained in the solubilizing detergent. However, more recently-detected binding of the CFTR C-terminus to multivalent PDZ-domain proteins (Hall et al., 1998; Wang et al., 1998; Short et al., 1998; Sun et al., 2000; Wang et al., 2000) could not have occurred with the truncated form. Therefore these original experiments could not have detected possible associations mediated by PDZ-domain proteins.

A second evaluation of CFTR quaternary structure came from an estimation of the cross-sectional area of freeze-fracture particles observed in membranes of *Xenopus* oocytes expressing CFTR (Eskandari et al., 1998). When compared with several other integral membrane proteins with known numbers of bilayer-spanning helices, the CFTR particle area corresponded more closely to 24 than 12 packed helices and hence it was concluded the CFTR may be dimeric in the membrane. There are several possible caveats to this interpretation, including the unknown helix packing arrangement and the possibility that all membrane-spanning sequences contributing to the particle area may not be from CFTR. In a third approach, the possibility that a homodimeric assembly forms the CFTR chloride channel was tested by expression of concatemers of two wild-type sequences or a wild type linked to an R-domain-deleted form (Zerhusen et al., 1999). Intermediate regulatory properties of the latter were interpreted as evidence of a chimeric channel formed by one wild-type and one mutant polypeptide. These regulatory properties were not very precisely defined, however, and there was no compelling evidence that the pore was formed by contributions from the two different CFTR sequences.

The issue of mediated rather than direct interactions between two CFTR polypeptides was raised by the finding that CFTR, like several other membrane receptors, transporters and channels (Fanning & Anderson, 1999; Garner, Nash & Huganir, 2000; Sheng & Sala, 2001) bound via its C-terminus to proteins containing multiple PDZ-domains (Hall et al., 1998; Short et al., 1998; Wang et al., 1998; Sun et al., 2000; Wang et al., 2000). Although physical complexes of more than one CFTR protein together with a PDZ-domain protein such as EBP-50 (ezrin binding protein 50) have not been directly demonstrated, stoichiometric titrations with bivalent forms of EBP-50 (Raghuram, Mak & Foskett, 2001) or another PDZ-domain protein, CAP70 (CFTR-associated protein 70 or PDZK1, (Kocher et al., 1999; Wang et al., 2000), were reported to increase the open probability of CFTR in membrane patches. These experiments have been interpreted as indicating that promotion of dimer formation increases channel activity.

Most recently Ramjeesingh et al. (2001) detected forms of CFTR of approximately monomeric and dimeric sizes in electrophoretic gels and gel filtration columns under partially dissociating conditions. In their experiments, the two forms did not exhibit significantly different protein kinase A-stimulated chloride flux, single-channel or ATPase activities and the significance of the larger species interpreted as containing two CFTR polypeptides was not elaborated upon.

We have now evaluated CFTR quaternary structure from endogenously and heterologously expressing cells by both biochemical and functional means and find no evidence of self-association of individual CFTR polypeptides to form homo-oligomeric structures.

Materials and Methods

Tissue Culture

BHK-21 (baby hamster kidney) cells were cultured as previously described (Loo et al., 1998). HEK293 cells were grown in DMEM (GIBCO-BRL) supplemented with 10% FBS, 1 mM glutamine, MEM nonessential amino acids, 1 mM sodium pyruvate, and 1% penicillin-streptomycin. Calu3 cells were grown in MEM (GIBCO-BRL), 10% FBS, 1 mM glutamine, 1 mM sodium pyruvate, and 1% penicillin-streptomycin. Clonal BHK-21 cells stably expressing wild type or ΔF508 C-terminally-tagged with HSV were generated by transfection by calcium phosphate (Sambrook & Russell, 2001), followed by growth and selection in DMEM-F12, 5% FBS, 1% penicillin-streptomycin, and 500 μM methotrexate. For transient transfection, cells at 70% confluence were transfected by calcium phosphate and harvested 48 hr post-transfection. All cells were grown at 37°C in 5% CO_2.

Velocity Gradient Centrifugation

Microsomal membranes from Calu3 and BHK cells stably expressing CFTR were isolated according to published protocols (Aleksandrov & Riordan, 1998). Membranes were solubilized in 1 ml of 0.09% NP-40, 0.2% Triton X-100, or RIPA (1% Triton X-100, 1% deoxycholic acid, and 0.1% SDS) in 150 mM NaCl and 50 mM Tris, pH 7.4 and layered on top of an 11-ml linear, continuous 10–36% sucrose gradient containing the respective detergent buffer. The sucrose gradient was formed by a gradient former (BioRad) and layered from the bottom to the top with a peristaltic pump (Buchler Instruments). Following centrifugation at 260,000 × *g* for 12 hr in an SW41Ti swing-out rotor (Beckman), twentyfour 500-μl fractions were collected from the top. Odd-numbered fractions were diluted with equal volume of RIPA buffer and immunoprecipitated with the CFTR monoclonal antibody M3A7 (1:250) (Kartner & Riordan, 1998) followed by protein G agarose beads (GIBCO-BRL), and blotted with the rabbit antibody 155 (1:1250). Molecular-weight markers IgM (950 kDa), thyroglobulin (660 kDa), urease (trimer, 272 kDa), catalase (240 kDa), and alkaline phosphatase (90 kDa) were diluted in 1 ml of 0.09% NP-40, 0.2% Triton X-100, or RIPA detergent buffer and sedimented as de-

scribed above. Peak migration of each species was determined by Coomassie staining of all fractions. The sucrose content of each fraction following centrifugation was measured by a handheld 0° to 10° Brix refractometer (Fisher) after a 1:3 sample dilution.

In Vitro Mutagenesis

The Flag M2 and HSV epitopes were introduced to either the C or N terminus of CFTR by PCR using primers encoding DYKDDDDK and QPELAPEDPED, respectively (single-letter amino acid) and cloned into full-length CFTR in pcDNA3 (Invitrogen) and pNUT vectors. To facilitate cloning, a NotI site was introduced immediately following the STOP codon for the C-terminal tags; a KpnI site was placed upstream of the Kozak sequence for the N-terminal tags. PCR primers for generating C-terminal M2 and HSV epitopes were 5′-GAA GAG ATG CAA GAT ACA AGG CTT GAC TAC AAG GAT GAC GAT GAC AAG TAG CGG CCG CAT-3′ and 5′-GAA GAG ATG CAA GAT ACA AGG CTT CAG CCT GAA CTC GCT CCA GAG GAT CCG GAA GAT TAG CGG CCG CAT-3′, respectively. PCR primers for generating N-terminal M2 and HSV epitopes (inserted between residues 1 and 2 of CFTR) were 5′-CTT GGT ACC CGA GAG ACC ATG GAC TAC AAG GAT GAC GAT GAC AAG CAG AGG TCG CCT CTG GAA AAGG-3′ and 5′-CTT GGT ACC CGA GAG ACC ATG CAG CCT GAA CTC GCT CCA GAG GAT CCG GAA GAT CAG AGG TCG CCT CTG GAA AAGG-3′, respectively. The ΔF508 mutation was cloned from pNUT-ΔF508 into C-terminally tagged CFTR by swapping the AflII-HpaI fragments. Missense mutations S341A and R347D were generated by site-directed mutagenesis (Stratagene) and cloned into CFTR-M2 by replacing the AflII-HpaI fragment, and into M2-CFTR by replacing the XbaI-HpaI fragment. The AflII-HpaI fragment containing TT338,339AA mutations (Linsdell et al., 1997) was substituted into CFTR-HSV in pcDNA3. The cloning description of the HA-tagged EPP-50 can be obtained from Chen and Riordan. Cloning was verified by restriction-enzyme digestion and sequencing by the Mayo Molecular Biology Core Facility.

Immunoprecipitation and Nickel-Affinity Binding

Cells transiently co-expressing M2- and HSV-tagged CFTR at either the C or N terminus were harvested with lysis buffer consisting of (in mM): 150 NaCl, 50 Tris, 10 $NaMoO_4$, and 0.09% NP-40, pH 7.4 supplemented with protease inhibitors E64 (3.5 μg/ml), benzamidine (157 μg/ml), aprotinin (2 μg/ml), leupeptin (1 μg/ml), and Pefabloc (480 μg/ml). Post-nuclear supernatant was immunoprecipitated with either M3A7 (1:250), anti-M2 (1:100, stock antiserum diluted with glycerol to 2 mg/ml, Sigma), anti-HSV (1:250 for C-terminal CFTR-HSV or 1:125 for N-terminal HSV-CFTR, Novagen), or the irrelevant anti-c-myc antibody 9E10 (1:250) overnight followed by 30 μl of packed protein G agarose beads for 2 hr at 4°C. Immune complexes were washed extensively with lysis buffer and eluted from protein G agarose beads with electrophoresis sample buffer. Immune precipitates were separated by SDS-PAGE and blotted with M3A7 (1:2500), anti-M2 (1:1000), anti-HSV (1:5000), or the anti-calnexin antibody K-9 (1:1000, kind gift from Dr. David Williams). BHK cells transiently co-expressing M2-CFTR, HSV-CFTR, and HA-EBP-50 were lysed in 0.09% NP-40 and analyzed as described above. EBP-50 signals were detected by Western blotting with 3F10 (1:2500). Immunoprecipitation experiments were also performed with other buffers containing 150 mM NaCl, 50 mM Tris, pH 7.4 and one of the following detergents: 1% *n*-octyl-β-D-glucopyranoside (OG, Calbiochem), 1% *n*-dodecyl-β-D-maltoside (DDM, Calbiochem), 0.1% $C_{12}E_8$ (Calbiochem), 0.2% $C_{10}E_6$ (Calbiochem), 0.2% Triton X-100, 1% digitonin, 1.5% 3-[(3-cholamidopropyl)dimethylammonio]-1-propanesulfonate (CHAPS), 0.2% lauryldimethyladmine oxide (LDAO, Calbiochem), and 0.15% zwittergent 3–14 (Calbiochem).

BHK cells stably expressing C-terminal polyhistidine-tagged CFTR were transiently transfected with either CFTR-M2 or CFTR-HSV and solubilized in lysis buffer consisting of 150 mM NaCl, 50 mM Tris, 25 mM imidazole, 0.09% NP-40, pH 8.0 and protease inhibitors. Post-nuclear supernatant was either immunoprecipitated with anti-M2 (1:100) or anti-HSV (1:250) followed by protein G agarose, or incubated with 30 μl packed Ni-NTA agarose beads (Qiagen) for 4 hr at 4°C. Ni-NTA beads were washed 6 times with solubilization buffer and eluted with lysis buffer containing 500 mM imidazole, pH 7.2 for 2 hr at 4°C. Residual proteins on Ni-NTA beads were washed off with electrophoresis sample buffer.

Cell Surface Labeling

BHK cells stably expressing CFTR-HSV were transfected with ΔF508-M2 and grown for 2 days at 37°C. Cells were incubated with 1 mg/ml EZ-link sulfo-NHS-LC-biotin (Pierce) in PBS, pH 8.0 supplemented with 0.1 mM $CaCl_2$ and 1.0 mM $MgCl_2$ for 30 min at 4°C. The reaction was quenched with glycine, BSA, and NH_4Cl for 30 min at 4°C. Cells were rinsed 6 times with PBS and lysed in 0.09% NP-40 buffer with protease inhibitors. Equal volume of post-nuclear supernatant was immunoprecipitated with either anti-M2 (1:100) or anti-HSV (1:250) followed by protein G agarose beads, or incubated with 50 μl packed immobilized streptavidin beads (Pierce) overnight. Bound complexes were eluted with electrophoresis sample buffer, fractionated by SDS-PAGE, and blotted with anti-M2 (1:1000) or anti-HSV (1:5000).

Single-Channel Measurements in Planar Lipid Bilayers

Single-channel recordings in planar lipid bilayers were performed according to published protocols (Gunderson & Kopito, 1995; Aleksandrov & Riordan, 1998). Briefly, microsomes from BHK-21 cells transiently expressing CFTR were pelleted and phosphorylated with 100 units/ml PKA (Promega) and 2 mM Na_2ATP (Sigma) at room temperature for 30 min in 10 mM HEPES, 5 mM $MgCl_2$, and 250 mM sucrose, pH 7.2. Membranes were added to the cis compartment of a Teflon cup separating the cis and trans compartments by a 0.2-mm aperture. Single channels were observed after the fusion of vesicles with a planar lipid bilayer consisting of 2:1 (wt:wt) 1-palmitoyl-2-oleoyl-*sn*-glycero-3-phosphoethanolamine: 1-palmitoyl-2-oleoyl-*sn*-glycero-3-phosphoserine (Avanti Polar Lipids) in *n*-decane painted onto the aperture. Channel measurements were made at 30°C in symmetric solutions containing (in mM): 300 Tris-HCl, 6 $MgCl_2$, and 1 EGTA, pH 7.2. To maximize channel openings, 5 mM Na_2ATP and 67 u/ml PKA were added to the cis compartment. Voltage potential is the difference between cis and trans (ground) compartments. Current measurements were performed under voltage-clamp conditions and filtered with an 8-pole Bessel low-pass filter with a corner frequency of 50 Hz and digitized at 500 Hz. pCLAMP 6.0 (Axon Instruments) and Origin 4.1 (Microcal) softwares were used for data analysis and fitting current-amplitude histograms.

To obtain approximately equal expression of different epitope-tagged CFTR-conduction variants, BHK cells were transiently cotransfected with cDNA in the following ratios: 6:1, S341A-M2:WT-HSV;7:5,R347D-M2:WT-HSV;1:1,S341A-M2:TT338, 339AA-HSV;3:11,R347D-M2:TT338,339AA-HSV;6:1,M2-S341A: HSV-WT; and 1:1,M2-R347D:HSV-WT. To determine the relative expression of each conduction species, equal volume of membrane

was solubilized in electrophoresis sample buffer and blotted with either anti-M2 or anti-HSV. To determine relative expression of each species, anti-HSV and anti-M2 signal intensities were normalized to M3A7 signal intensities for each conjugated CFTR species. The normalizing factor of anti-M2:anti-HSV for C-terminally-tagged CFTR was 0.33 obtained from the ratio CFTR-$M2_{anti\text{-}M2}$/CFTR-$M2_{M3A7}$*CFTR-HSV_{M3A7}/CFTR-$HSV_{anti\text{-}HSV}$ with respective values (in OD·mm) 0.98, 0.34, 0.28, and 2.48. Similarly, for N-terminally-tagged CFTR, the normalizing factor of anti-M2:anti-HSV was 1.36, obtained from the ratio M2-$CFTR_{anti\text{-}M2}$/M2-$CFTR_{M3A7}$*HSV-$CFTR_{M3A7}$/HSV-$CFTR_{anti\text{-}HSV}$, with respective values (in OD·mm) 2.10, 1.96, 1.19, and 0.94. Gel scanning and image analysis were performed with Quantity One (PDI).

Results

Velocity-Gradient Centrifugation of Detergent-Solubilized CFTR

As one means of estimating the molecule's size and thereby its oligomeric state, the protein solubilized from membranes of BHK cells in which it was heterologously expressed (Loo et al., 1998), was subjected to velocity sedimentation in linear, continuous sucrose gradients. Mild conditions were employed to minimize disruption of protein-protein interactions. The non-ionic NP-40 at a low concentration was previously found to be suitable for this purpose, as it maintained the delicate association between nascent CFTR and the molecular chaperone, Hsp90 (Loo et al., 1998). Under these conditions, mature CFTR migrated as a sharp peak in 3 of 12 fractions examined (Fig. 1*A*, left panel). The center of this peak at fraction 6 corresponds to an M_r of approximately 130 kDa relative to the migration of standards (Fig. 1*C*, left panel). When another non-ionic detergent was employed at a relatively low concentration (0.2% Triton X-100), there was migration to a slightly higher sucrose density corresponding to an M_r in the 200 kDa range, possibly reflecting the binding of more of this detergent. Significantly, however, migration was not substantially altered under the much stronger dissociating conditions of RIPA buffer (Fig. 1*A*, right panel) and 1% SDS (*data not shown*). From the size estimates obtained by interpolation from the standard curves, these observations indicate that the bulk of CFTR in the BHK cell membranes is monomeric. It is abundantly clear from these blots and even at much longer exposures that no larger species representing oligomers or aggregates are detected at higher fraction numbers. This is also true when CFTR was heterologously co-expressed with EBP-50 (*data not shown*).

Although the reports interpreting CFTR as dimeric also employed heterologous expression systems (Eskandari et al., 1998; Zerhusen et al., 1999; Wang et al., 2000), it is possible that conditions or factors required for self-association were not ideal in BHK cells. Therefore the same types of experiment were performed employing membranes from Calu-3 epithelial cells in which CFTR is endogenously expressed and functions as a secretory chloride channel (Haws et al., 1994; Shen et al., 1994). Figure 1*B* shows that the sedimentation is nearly identical under all three solubilizing conditions as it was in the case of the recombinant protein. Hence, even in the assumed native state where all requirements of normal CFTR function are fulfilled, including the presence of such things as PDZ-domain proteins that might tether C-termini of two CFTRs together, the bulk species present would appear to be a monomer.

The observations do not exclude the possibility that multiple CFTR glycoproteins might assemble by interactions that are disrupted even by mild solubilizing conditions. In that case, such interactions might be expected to be captured by chemical cross-linking and this approach is addressed in a separate study (Chen and Riordan, unpublished data).

Co-Expression of Differentially Epitope-tagged CFTR Species

Our initial co-immunoprecipitation experiments were conceptually analogous to those of Marshall et al. (1994) in that the co-expressed species had different C-termini. In their case, a segment of the C-terminus was simply absent from one of the species, whereas we attached different epitope tags to the C-terminus of full-length CFTR. This modification did not alter either the processing or function of the molecule. Both of these strategies, however, preclude the association of the two CFTRs by a bivalent PDZ-domain protein and perhaps not surprisingly, no association was detected. This is apparent from the immunoprecipitation experiment depicted in Fig. 2. When expressed separately, the M2- and HSV-tagged species were detected only by the antibody recognizing its epitope (Fig. 2*A*) and this remained true when the two were co-expressed (Fig. 2*B*). This finding demonstrates the lack of strong interactions between parts of the protein other than the C-terminus. As an internal test for a co-immunoprecipitation, calnexin, an ER-membrane chaperone that binds nascent CFTR molecules (Pind, Riordan & Williams, 1994) is detected in these immunoprecipitates at ratios approximating that of immunoprecipitated CFTR (Fig. 2*B*, *compare* M3A7 and anti-CNX blots). This was further confirmed by the finding that neither of the C-terminally epitope-tagged species were present in the Ni-NTA-bound fraction together with a polyhistidine-tailed CFTR when they were co-expressed with it (Fig. 2*C*).

To determine if associations might occur when the C-termini were free to participate, similar experiments were performed but with the epitopes fused at the N-termini rather than the C-termini (Fig. 2*D*).

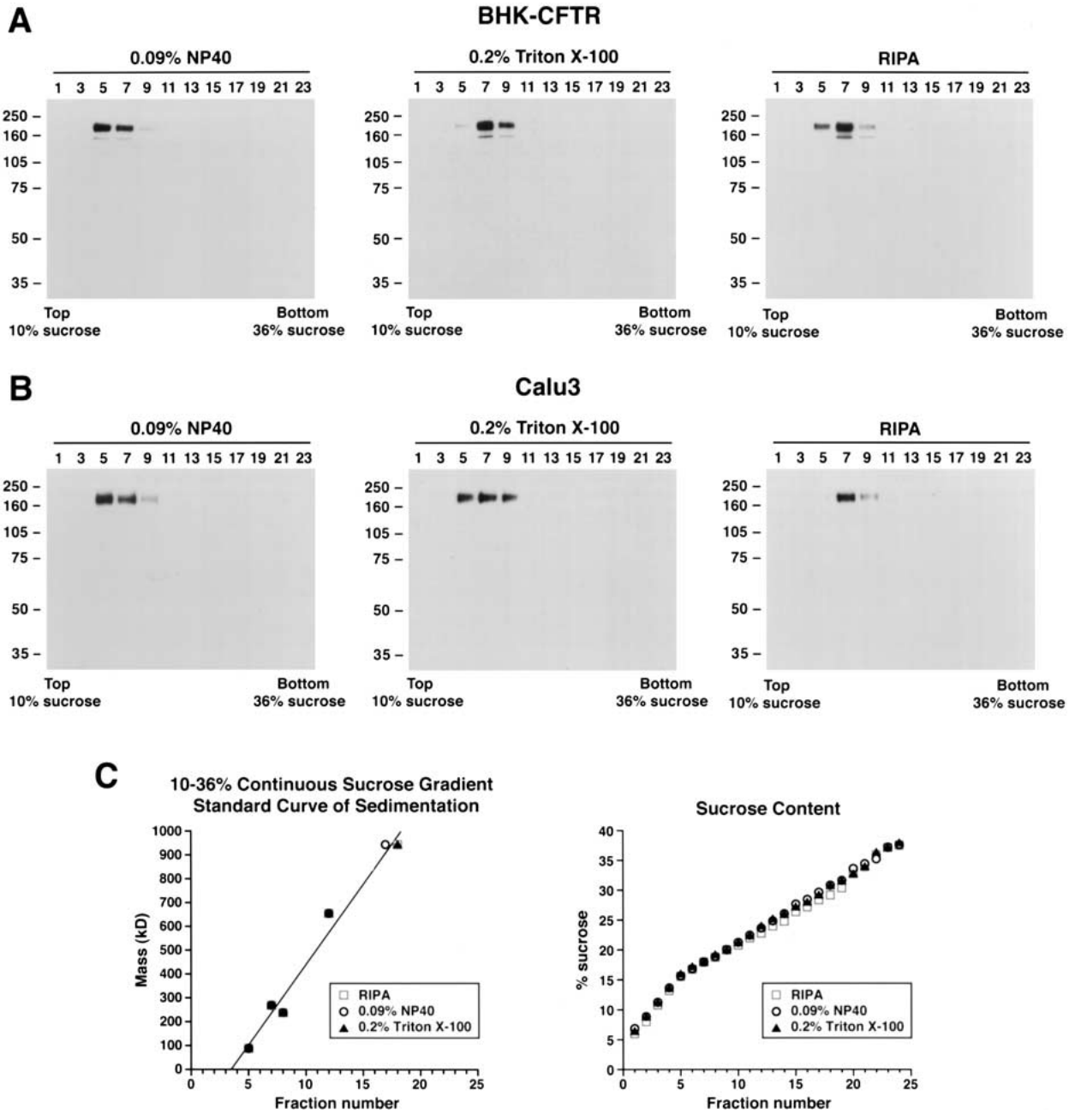

Fig. 1. CFTR sediments as a monomer in 10–36% linear, continuous sucrose gradients. Microsomal membranes from (*A*) BHK cells heterologously expressing CFTR and from (*B*) Calu3 cells endogenously expressing CFTR were solubilized in 1 ml of 0.09% NP-40, 0.2% Triton X-100, or RIPA (0.7 to 1.0 mg/ml protein) and layered on top of an 11-ml linear, continuous 10–36% sucrose gradient containing the respective detergent buffer. Following centrifugation at 260,000 × *g* for 12 hr, twentyfour 500-μl fractions were collected from the top. CFTR in odd-numbered fractions was immunoprecipitated with M3A7 (1:250) and blotted with antibody 155 (1:1250). Following centrifugation, the linearity of the sucrose gradient was confirmed by quantifying sucrose content by refraction. In all conditions, CFTR sediments between fractions 5–9. (*C*) Standard curve derived from the sedimentation of molecular weight standards in 10–36% linear, continuous sucrose gradient containing 0.09% NP-40, 0.2% Triton X-100, or RIPA: IgM (950 kDa), thyroglobulin (660 kDa), urease (trimer, 272 kDa), catalase (240 kDa), and alkaline phosphatase (90 kDa).

However, as shown in Fig. 2*E*, the two species differentially tagged at the N-termini did not co-immunoprecipitate either. This was also seen when the two N-terminally tagged species were co-expressed with EBP-50 (Fig. 2*F*). Despite possessing a strong in vitro binding interaction, an association between CFTR and the PDZ-domain protein was detected only when excess amounts of immunoprecipitating antibodies were used, indicating that their association may be compartmentalized or dynamically

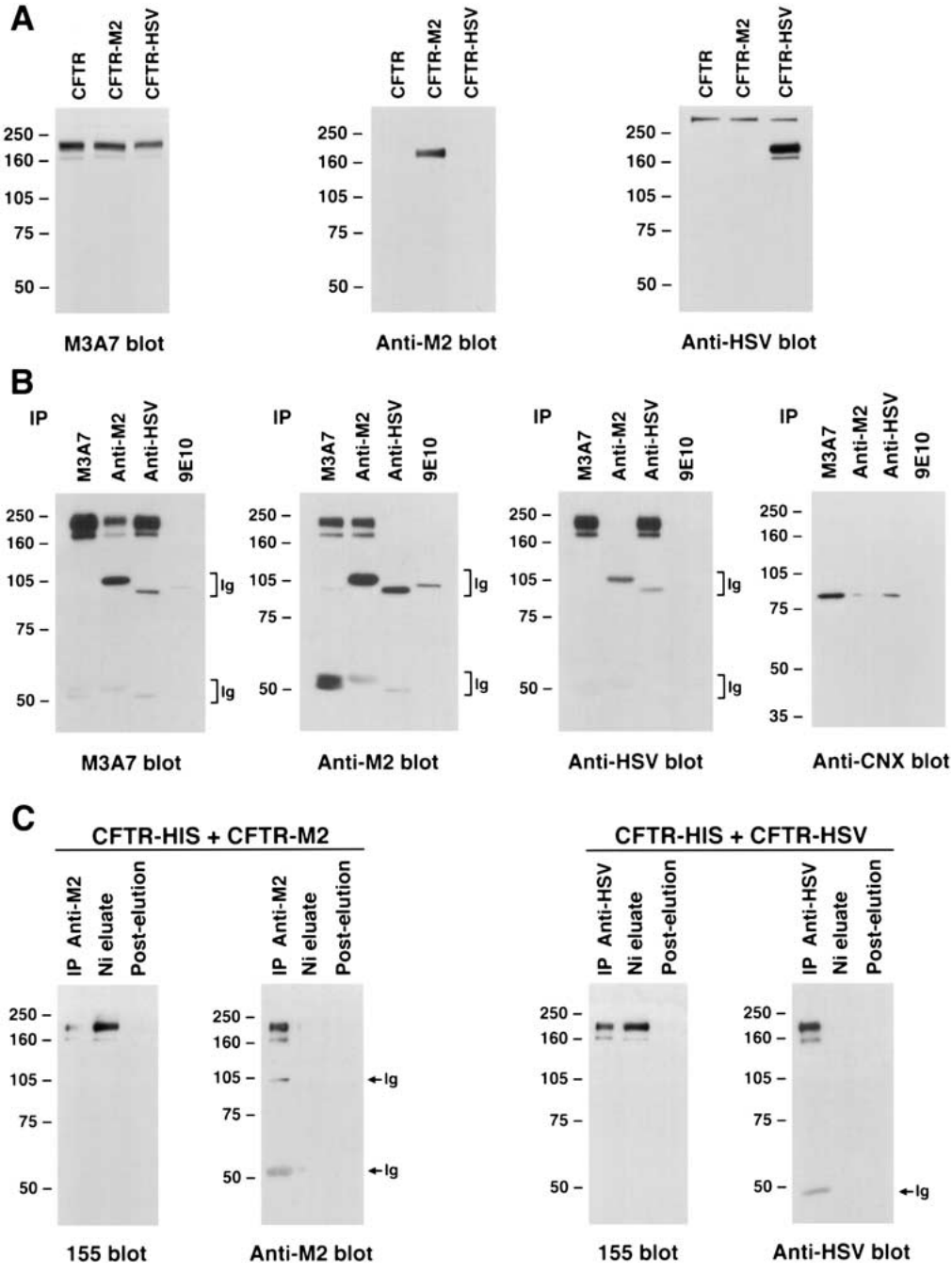

Fig. 2. No detectable association between different epitope-tagged CFTR species by immunoprecipitation and nickel affinity binding. (*A*) Lysates of BHK cells expressing wild-type and C-terminally M2 and HSV epitope-tagged CFTR (CFTR, CFTR-M2, and CFTR-HSV, respectively). Cell lysates (45 μg per lane) were blotted with M3A7 (1:2500), anti-M2 (1:1000), or anti-HSV (1:5000). The tagged constructs are recognized specifically by their corresponding antibody. (*B*) BHK cells transiently co-expressing CFTR-M2 and CFTR-HSV were solubilized in 0.09% NP-40 and immunoprecipitated with M3A7 (1:250), anti-M2 (1:100), anti-HSV (1:250), or the irrelevant antibody 9E10 (1:250). No co-immunoprecipitation of CFTR-M2 and CFTR-HSV is seen (lane *3*, anti-M2 blot and lane *2*, anti-HSV blot). As an internal control for a co-immunoprecipitation, calnexin is detected in these immunoprecipitates. (*C*) BHK cells stably expressing polyhistidine-tagged CFTR were transiently transfected with CFTR-M2 or CFTR-HSV and solubilized in 0.09% NP-40. Postnuclear supernatant was either immunoprecipitated with anti-M2 (1:100) or anti-HSV (1:250), or incubated with Ni-NTA agarose beads. Bound CFTR was eluted with 500 mM imidazole. Residual CFTR was washed off with sample buffer. No detectable association between CFTR-M2 and CFTR-HSV with polyhistidine-tagged CFTR is evident (lane *2*, anti-M2 and anti-HSV blots).

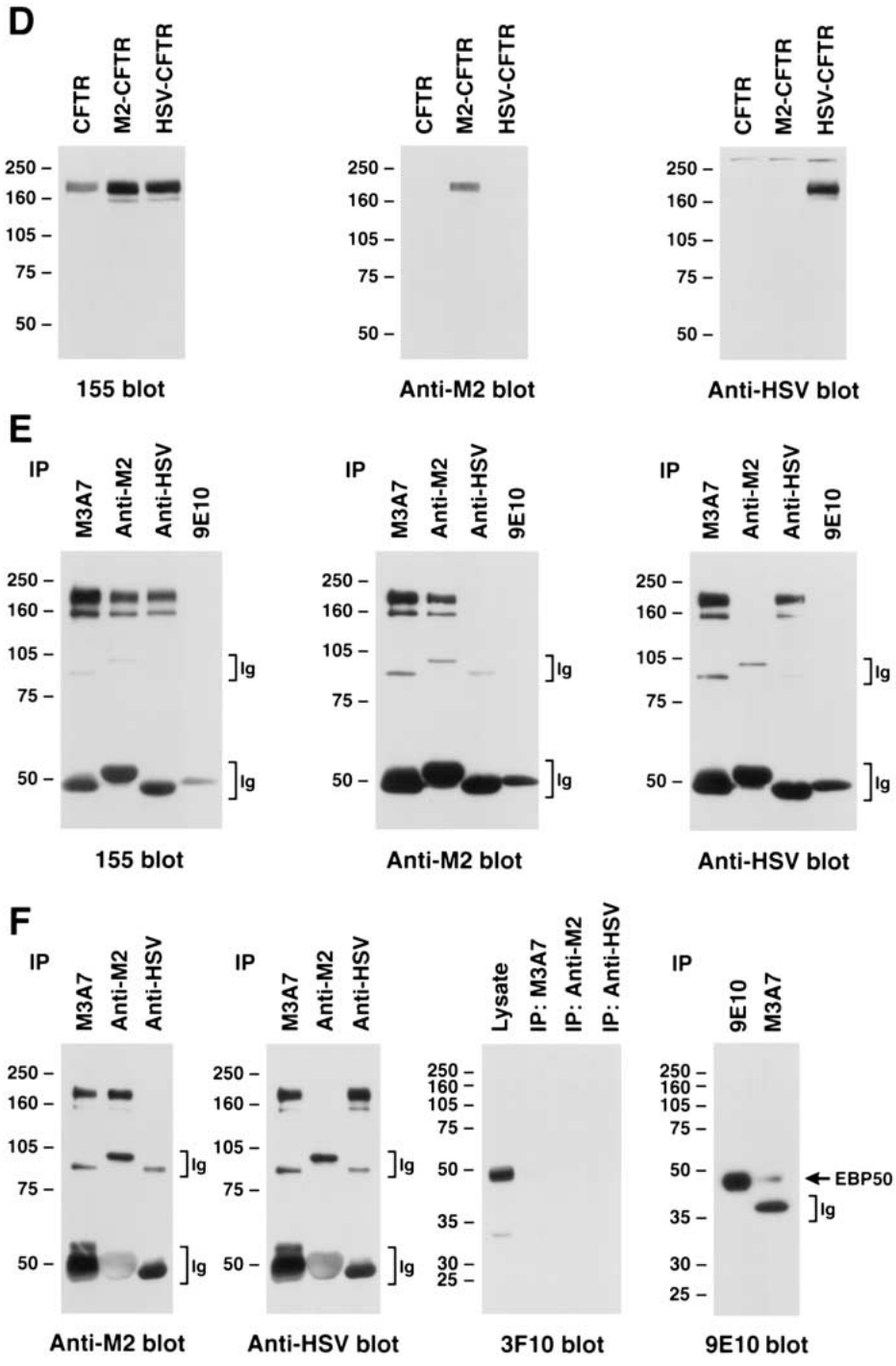

Fig. 2. (*Continued*). (*D*) Lysates of BHK cells expressing wild-type and N-terminally M2 and HSV epitope-tagged CFTR (CFTR, M2-CFTR, and HSV-CFTR, respectively). Cell lysates (45 μg per lane) were blotted with M3A7 (1:2500), anti-M2 (1:1000), or anti-HSV (1:5000). The tagged constructs are recognized specifically by their corresponding antibody. (*E*) BHK cells transiently co-expressing M2-CFTR and HSV-CFTR were lysed in 0.09% NP-40 and immunoprecipitated with M3A7 (1:250), anti-M2 (1:100), anti-HSV (1:125), or the irrelevant antibody 9E10 (1:250). No co-immunoprecipitation of M2-CFTR and HSV-CFTR is seen (lane *3*, anti-M2 blot and lane *2*, anti-HSV blot). (*F*) M2-CFTR and HSV-CFTR co-expressed with HA-tagged EBP-50 in BHK cells were lysed in 0.09% NP-40 and immunoprecipitated with M3A7 (1:250), anti-M2 (1:100), and anti-HSV (1:100). Immunoprecipitates were blotted with anti-M2 (1:1000), anti-HSV (1:5000), and 3F10 (1:2500). Lane *1* of the 3F10 blot contains 10 μg of cell lysate. To demonstrate an association between CFTR and EBP-50, BHK cells co-expressing CFTR and EBP-50 C-terminally tagged with c-myc were lysed in 0.09% NP-40 and immunoprecipitated with M3A7 (1:67) and 9E10 (1:67). EBP-50 signal was detected by Western blotting with 9E10 (1:2500). The M3A7 immunoprecipitates were loaded at eight times the volume of 9E10 immunoprecipitates.

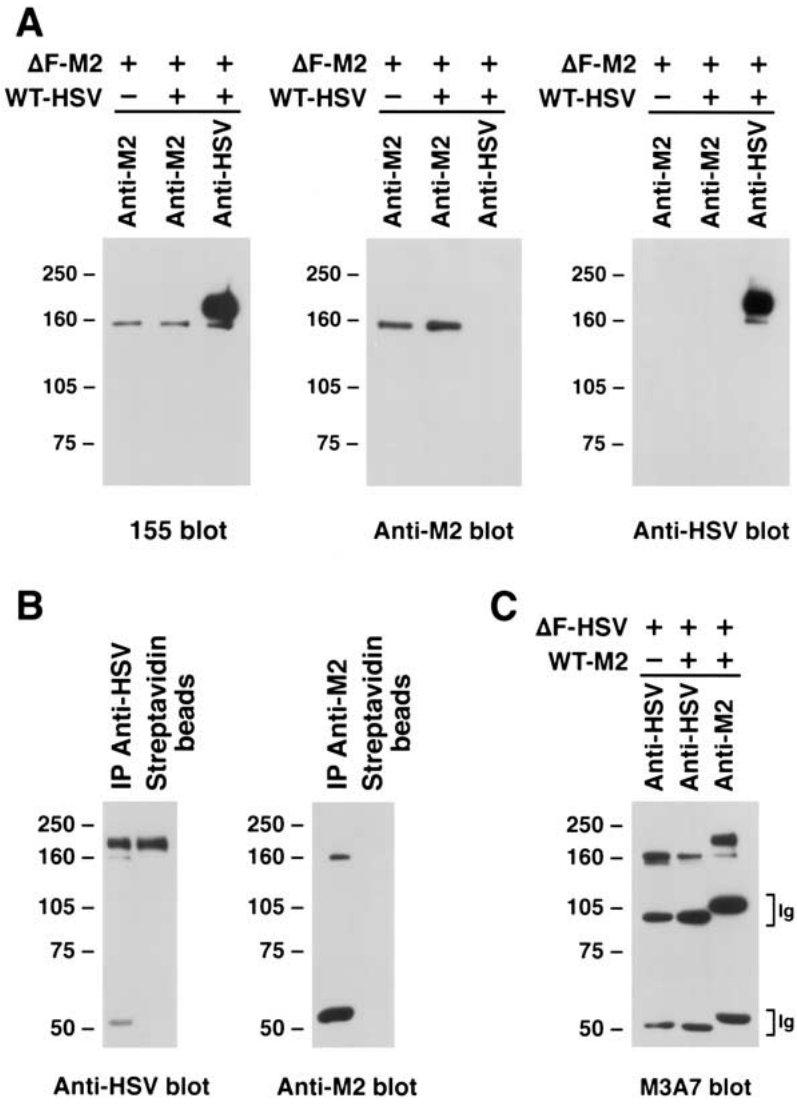

Fig. 3. Co-exressed epitope-tagged wild-type and ΔF508 CFTR do not co-assemble or influence each other's maturation (*A*) Parental BHK cells and BHK cells stably expressing WT-HSV were transiently transfected with ΔF508-M2 and grown for 48 hours at 37°C. Cells were lysed in 0.09% NP-40 and immunoprecipitated with anti-M2 (1:100) and anti-HSV (1:250). ΔF508-M2 does not acquire complex glycosylation in the presence or absence of wild-type CFTR (lanes *1* and *2*, 155 blot). In addition, ΔF508-M2 and WT-HSV do not co-immunoprecipitate (lane *3*, anti-M2 blot and lane *2*, anti-HSV blot). (*B*) Cells co-expressing ΔF508-M2 and WT-HSV as in (*A*) were surface-biotinylated and lysed in 0.09% NP-40. Postnuclear supernatant was either immunoprecipitated with anti-M2 (1:100) or anti-HSV (1:250), or incubated with immobilized streptavidin beads. Whereas the mature WT-HSV is surface-labeled (lane *2*, anti-HSV blot), neither ΔF508-M2 nor immature WT-HSV are labeled (lane *2*, anti-M2 blot and lane *2*, anti-HSV blot). (*C*) BHK cells stably expressing ΔF508-HSV were lysed in 0.09% NP-40 and immunoprecipitated with anti-HSV (1:250). ΔF508-HSV is core-glycosylated (lane *1*) with an additional smaller CFTR species due either to an alternative translation initiation site or a proteolytic cleavage of a small N-terminal fragment. ΔF508-HSV-expressing cells were transiently transfected with WT-M2 and grown for two days at 37°C. Cells were solubilized in 0.09% NP-40 and immunoprecipitated with anti-HSV (1:250) or anti-M2 (1:100). Neither the retention of WT-M2, as evident by the normal ratio of mature and immature CFTR signal intensities (lane *3*), nor maturation of ΔF508-HSV (lane *2*) are seen.

regulated (Fig. 2*F*). This may account for an undetectable amount of PDZ-mediated associating CFTR molecules, as had also been reported by Wang et al. (2000). Hence, as in the velocity gradient sedimentation experiments, individual CFTR polypeptides solubilized from membranes in mild detergent show no propensity to associate with each other.

The lack of association between the two immunologically-different CFTR species was also evident in other experimental conditions (*data not shown*), including co-expression in HEK293 cells, complete immunoprecipitation of CFTR using excess amounts of anti-M2 and anti-HSV antibodies, and solubilization of CFTR in other mild nonionic and zwitterionic detergent buffers including 0.1% $C_{12}E_8$, 0.2% $C_{10}E_6$, 0.2% Triton X-100, 1% OG, 1% DDM, 1% digitonin, 0.15% zwittergent 3-14, 0.2% LDAO, and 1.5% CHAPS. To test the possibility that CFTR may associate to form transient complexes when activated (Wang et al., 2000; Schillers et al., 2001), we treated BHK cells co-expressing C- or N-terminally-tagged CFTR with forskolin prior to solubilization; no association was evident by immunoprecipitation following CFTR stimulation (*data not shown*).

Co-Assembly of Wild-type and ΔF508 CFTR is not Detected

CFTR is a glycoprotein that is biosynthetically processed through the secretory pathway. At the endoplasmic reticulum (ER), CFTR is core-glycosylated at two asparagine residues in the fourth extracellular loop (Chang et al., 1994; Cheng et al., 1990; Gregory et al., 1990; Hämmerle et al., 2000). Following conformational maturation at the ER (Lukacs et al., 1994), CFTR is transported to the Golgi apparatus where its oligosaccharide chains undergo mannose trimming and complex glycosylation. These different glycosylation states provide facile assessment of the state of CFTR processing and trafficking by western

blotting (Fig. 3). The biosynthesis of CFTR at the ER is stringently regulated as ~20–30% of newly synthesized wild-type CFTR proteins acquire a mature conformation (Lukacs et al., 1994). Since subunit assembly at the ER is a component in the biosynthetic maturation of oligomeric proteins (Hurtley & Helenius, 1989; von Heijne, 1997), we assayed for CFTR structure by co-expressing two CFTR molecules with different maturation capabilities. In a report indicating that P-gp oligomerizes, its assembly occurred at the ER (Poruchynsky & Ling, 1994).

We monitored the biosynthetic processing of wild-type and the CF mutant ΔF508 CFTR in co-expression studies to test for possible CFTR assembly at the ER. Virtually all ΔF508 proteins are retained at the ER where it is cotranslationally poly-ubiquitinated and degraded (Jensen et al., 1995; Ward, Omura & Kopito, 1995; Sato, Ward & Kopito, 1998). If CFTR were oligomeric, wild-type CFTR might "rescue" the ΔF508 protein to the cell surface by assembly at the ER; equally likely, CFTR oligomers containing ΔF508 and wild-type CFTR might be retained at the ER. Wild-type and ΔF508 molecules were epitope-tagged at their C termini to differentiate each species. To study whether wild-type CFTR can promote ΔF508 expression at the plasma membrane, BHK cells stably expressing WT-HSV were transiently transfected with ΔF508-M2 and grown for two days at 37°C prior to solubilization and immunoprecipitation with anti-M2 and anti-HSV antibodies. When co-expressed with WT-HSV, ΔF508-M2 did not acquire complex glycosylation or associate with WT-HSV by immunoprecipitation (Fig. 3*A*). Addressing the possibility that ΔF508 can reach the plasma membrane in the absence of complex glycosylation, surface biotinylation on cells co-expressing WT-HSV and ΔF508-M2 labeled the mature form of wild type, but not ΔF508 (Fig. 3*B*). As an internal control, the immature ER-resident form of WT-HSV was not biotinylated. To assess the influence of ΔF508 on the biosynthesis of wild-type CFTR, WT-M2 was transiently expressed in BHK cells stably expressing ΔF508-HSV for two days at 37°C. Neither the retention of the wild-type protein, as evident by the normal ratio of complex and core-glycosylated CFTR band intensities, nor the acquisition of complex glycosylation by ΔF508 were seen (Fig. 3*C*). While the possibility that wild-type and ΔF508 CFTR nascent chains associate in the ER is not excluded by these observations, they do show that if this does occur it is without influence on the ability of either to progress through the secretory pathway.

Co-Expression of CFTR Variants with Different Unitary Conductances

The sixth transmembrane helix of CFTR has a profound influence on chloride conductance (Dawson, Smith & Mansoura, 1999). Mutations S341A and R347D (single-letter amino acid) dramatically lower chloride conductance (Tabcharani et al., 1993; McDonough et al., 1994) while the double mutation TT338, 339AA enhances chloride conduction (Linsdell et al., 1997). Because most oligomeric pore-forming proteins organize their subunits around the pore (Song et al., 1996; Chang et al., 1998; Doyle et al., 1998; Koronakis et al., 2000), we tested whether CFTR is monomeric or oligomeric by analyzing the population of channel conductances from cells co-expressing two conduction variants. An oligomeric channel comprised of different subunits each with a different channel conductance should exhibit a hybrid conductance that is intermediate to those of the two constituents (Cooper, Couturier & Ballivet, 1991). In contrast, two co-existing monomers should simply reveal two discrete conductance populations.

To monitor the expression of each species in co-expression experiments, we coupled the M2 and HSV epitopes to either the C or N terminus of CFTR. These epitope tags have negligible effects on CFTR conductance as all channels displayed slight outward rectification measuring ~14 pS and ~10 pS at negative and positive potentials, respectively (Fig. 4*A*, 4*B*, 5*A*, and 5*B*). In these bilayer experiments only those CFTR channels whose NBDs face the cis compartment containing MgATP are active. Thus, positive currents are outwardly directed currents. Although we did not extensively characterize the single-channel kinetics of these epitope-tagged CFTR proteins, they were indistinguishable from unmodified CFTR channels (Aleksandrov & Riordan, 1998). From 3-minute continuous single-channel recordings with 5 mM MgATP at 30°C, mean open and closed times were: τ_o = 176 msec τ_c = 174 msec with the N-terminal M2 epitope and τ_o = 177 msec, τ_c = 160 msec with the HSV epitope. This is different from the report by Chan et al. (2000) whose M2-tagged CFTR channels possessed a slower opening rate and lower open channel probability. Factors contributing to these differences may include different experimental conditions (for example a temperature of 30°C in our experiments versus 21–23°C in theirs) and the substitution of the residue immediately following the M2 epitope (second residue of wild-type CFTR) from glutamine to leucine by Chan et al. Also our measurements were made in planar lipid bilayers where conditions are not identical to those in *Xenopus* oocyte membranes where theirs were made.

To the C-terminal ends of CFTR, we attached the M2 epitope to S341A and R347D and the HSV epitope to wild type and TT338, 339AA (S341A-M2, R347D-M2, WT-HSV, and TT338, 339AA-HSV, respectively). Single-channel chord conductances for S341A-M2, R347D-M2, WT-HSV, and TT338, 339AA-HSV at −100 mV were (in pS): 2.2, 5.1, 14.3, and 15.6, respectively (Figs. 4*C* and 4*D*). The relative conductance

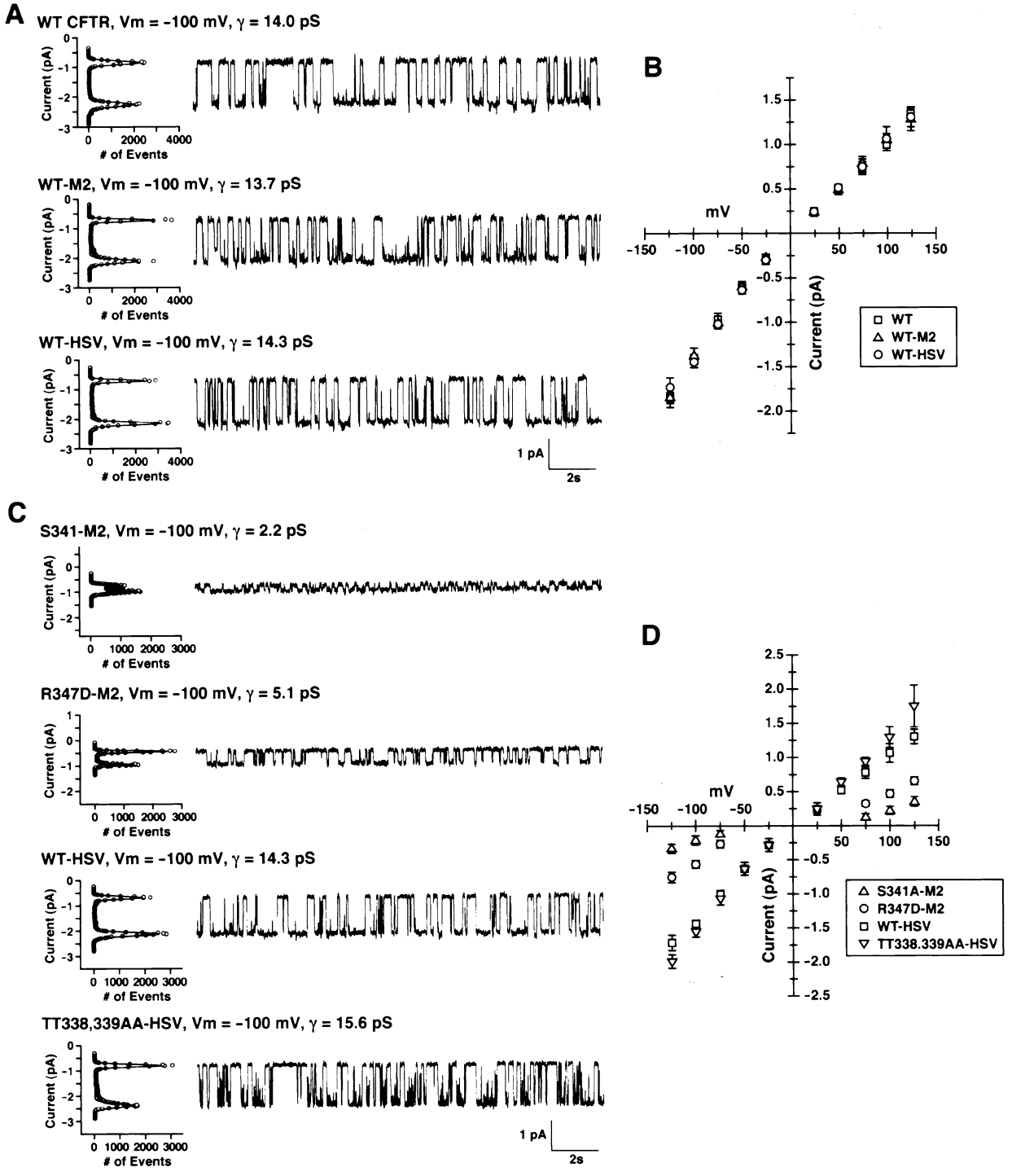

Fig. 4. No detectable hybrid conducting channel from microsomal vesicles containing two C-terminally-tagged CFTR pore variants. Single-channel measurements of microsomes from BHK cells transiently expressing CFTR are described in Materials and Methods. CFTR-containing membranes were phosphorylated with the catalytic subunit of PKA. All channel measurements were performed under voltage-clamp conditions at 30°C in symmetric buffer containing (in mM): 300 Tris-HCl, 6 $MgCl_2$, 1 EGTA, pH 7.2; 5 mM Na_2ATP and 67 u/ml PKA were added to the cis compartment to maximize channel activity. Current is measured with the trans compartment grounded. (*A*) Amplitude histograms and single-channel recordings of unmodified and C-terminally M2- and HSV-tagged CFTR (WT, WT-M2, and WT-HSV, respectively). All channels display similar single-channel kinetics and open-channel probabilities. CFTR channels possess a conductance of $\sim$ 14pS at -100 mV. (*B*) Single-channel current-voltage relationships of WT, WT-M2, WT-HSV. All channels display a slight outward rectification of current. (*C*) Amplitude histograms and single-channel recordings of low-conduction mutants S341A and R347D C-terminally tagged with M2 (S341A-M2 and R347D-M2, respectively), and high-conduction variants WT and TT338, 339AA C-terminally tagged with HSV (WT-HSV and TT338, 339AA-HSV, respectively). At a holding potential of -100 mV, single-channel conductances are 2.2, 5.1 14.3, and 15.6 pS, respectively. (*D*) Single-channel current-voltage relationships of S341A-M2, R347D-M2, WT-HSV, and TT338,339A-HSV.

E

Co-Expression of S341A-M2 and WT-HSV

	Number of Channels		Number of Channels	Total # of Channels
2 pS	70	14 pS	87	165
		9.5 pS	5	95% CI = 0 - 2.2%
		7.5 pS	3	
	70		95	
	42.4%		57.6%	

S341A-M2 WT-HSV

0.351 OD x mm 1.065 OD x mm
50.2% 49.8%

Co-Expression of R347D-M2 and WT-HSV

	Number of Channels		Number of Channels	Total # of Channels
5 pS	70	14 pS	85	163
		9.5 pS	3	95% CI = 0 - 2.2%
		7.5 pS	5	
	70		93	
	42.9%		57.1%	

R347D-M2 WT-HSV

0.368 OD x mm 1.133 OD x mm
49.8% 50.2%

Co-Expression of S341A-M2 and TT338,339AA-HSV

	Number of Channels		Number of Channels	Total # of Channels
2 pS	107	16 pS	56	170
		8 pS	7	95% CI = 0 - 2.2%
	107		63	
	62.9%		37.1%	

S341A-M2 TT338,339AA-HSV

0.722 OD x mm 1.314 OD x mm
62.7% 37.3%

Co-Expression of R347D-M2 and TT338,339AA-HSV

	Number of Channels		Number of Channels	Total # of Channels
5 pS	84	16 pS	61	154
2 pS	1	12 pS	4	95% CI = 0 - 2.4%
		8 pS	4	
	85		69	
	55.2%		44.8%	

R347D-M2 TT338,339AA-HSV

0.499 OD x mm 1.506 OD x mm
50.3% 49.7%

Fig. 4. (*Continued*). (*E*) Tabulation of single-channel conductances from microsomes containing a low-conducting (S341A.M2 or R347D-M2) and a high-conducting species (WT-HSV or TT338,339AA-HSV). Holding potential was −100 mV. The relative expression of each co-expressed species was determined by densitometry as described in Materials and Methods. No hybrid-conducting channel is detected (95% CI ≤ 2.4% in all combinations).

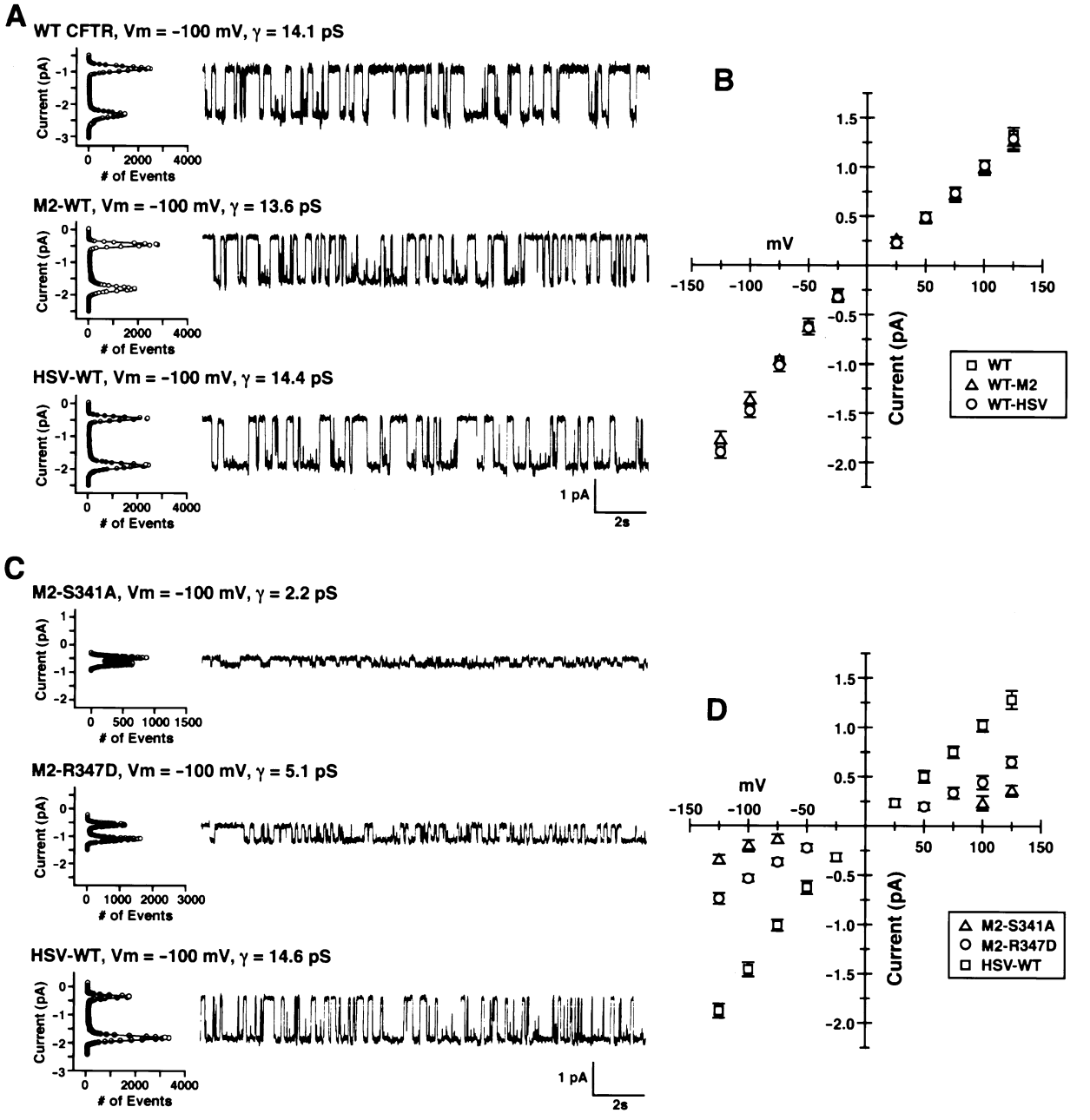

Fig. 5. No detectable hybrid conducting channel from microsomal vesicles containing two N-terminally-tagged CFTR pore variants. Single-channel measurements of microsomes from BHK cells transiently expressing CFTR as described in Fig. 4. (*A*) Amplitude histograms and single-channel recordings of unmodified and N-terminally M2- and HSV-tagged CFTR (WT, M2-WT, and HSV-WT, respectively). All channels display similar single-channel kinetics and open-channel probabilities. CFTR channels possess a conductance of ~14pS at −100 mV. (*B*) Single-channel current-voltage relationships of WT, M2-WT, and HSV-WT. All channels display a slight outward rectification of current. (*C*) Amplitude histograms and single-channel recordings of S341A and R347D N-terminally tagged with M2 (M2-S341A and M2-R347D, respectively), and WT N-terminally tagged with HSV (HSV-WT). Single-channel conductances at −100 mV are 2.2, 5.1, and 14.6 pS, respectively. (*D*) Single-channel current-voltage relationships of M2-S341A, M2-R347D, and HSV-WT.

of each to HSV-WT is in close agreement with reported values (Tabcharani et al., 1993; McDonough et al., 1994; Linsdell et al., 1997). To assess CFTR stoichiometry, we co-expressed approximately equal amounts of a low-(S341A-M2 or R347D-M2) and a high-conduction species (WT-HSV or TT338,339AA-HSV) for single-channel analysis (Fig. 4*E*). To maximize channel kinetics, all recordings were made in the presence of 5 mM MgATP and PKA at 30°C. In all combinations, the majority of observed conduc-

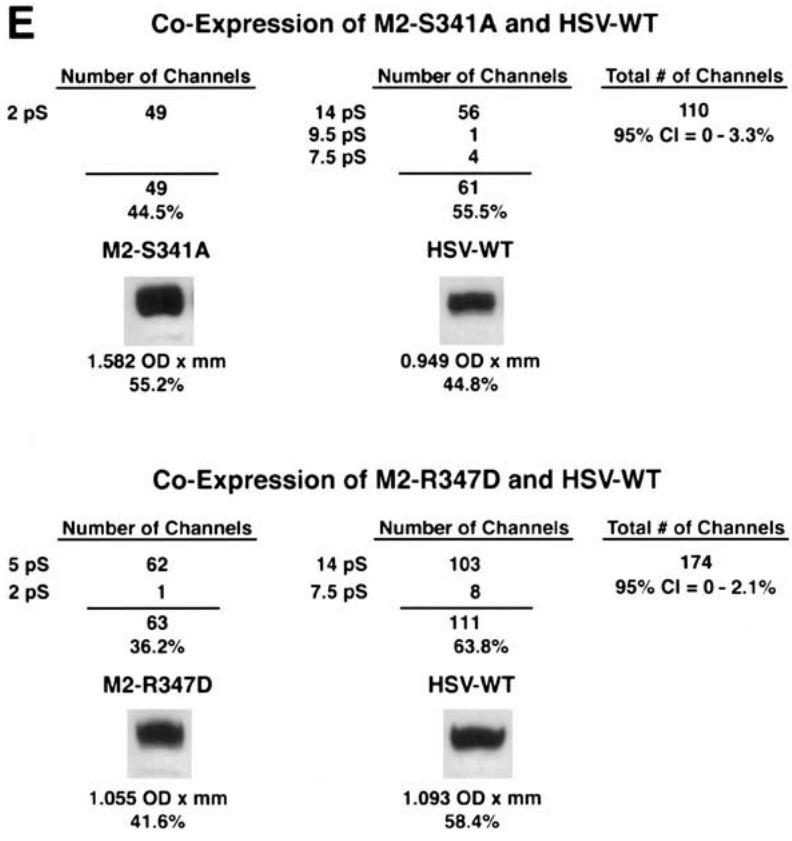

Fig. 5. (*Continued*). (*E*) Tabulation of single-channel conductances from microsomes containing HSV-WT and either M2-S341A or M2-R347D. Holding potential was −100 mV. The relative expression of each co-expressed species was determined by densitometry as described in Material and Methods. Co-expressed CFTR proteins do not form a hybrid channel (95% CI ≤ 3.3% for M2-S341A and HSV-WT, and ≤ 2.1% for M2-R347D and HSV-WT).

tances was comprised of each co-expressed conduction species. Intermediate conducting channels were infrequently observed; membrane vesicles containing WT-HSV plus S341A-M2 or R347D-M2 produced 9.5 pS and 7.5 pS channels, and vesicles containing TT338,339AA-HSV plus S341A-M2 or R347D-M2 yielded 12 pS, 8 pS, and 2 pS channels. These channels were most likely subconductances of WT-HSV (9.5 pS and 7.5 pS channels), TT338,339AA-HSV (12 pS and 8 pS), and R347D-M2 (2 pS) since they were seen with microsomes containing each of these species alone. Moreover, the same subconductance states of WT-HSV and TT338,339AA-HSV were seen when each was co-expressed with a different low-conduction species. The 7.5 pS (WT-HSV) and 8 pS (TT338, 339AA-HSV) conductances possessed very fast channel kinetics and interconverted with the main conductance state. The 95% confidence interval (CI) that the intermediate conducting channels were the products of co-assembled pore variants was ≤ 2.4% in all cases. The low frequency of intermediate conducting channels favored a binomial distribution of monomeric, but not oligomeric CFTR channels, given random assembly of subunits. In each experiment, the relative appearance of each co-expressed species closely approximated its relative expression level (*see* Materials and Methods).

Similar results were seen when these pore variants were epitope-tagged at their N termini. The chord conductances of M2-S341A, M2-R347D, and HSV-WT at −100 mV (in pS) were 2.2, 5.1, and 14.6, respectively (Fig. 5*C* and 5*D*). When co-expressed, microsomes containing HSV-WT and either M2-S341A or M2-R347D produced conductances that were predominantly channels of each constituent in their main conductance states and infrequently their subconductance states (Fig. 5*E*). The possibility that these intermediate conductances resulted from a hybrid assembly of multiple CFTR molecules was ≤ 3.3% and ≤ 2.1% for HSV-WT plus M2-S341A and M2-R347D, respectively. Similarly, the low frequency of intermediate-conducting channels favored a monomeric CFTR structure, with relative appearance of each co-expressed channel species closely matching its relative expression level. Similar results were seen when these pore variants in the absence of epitope-tagging were co-expressed, although their relative expression levels could not be quantified (*data not shown*).

Hence we conclude that two CFTR polypeptides do not assemble to form a single pore. These single-channel data per se, however, do not preclude assembly of two polypeptides where each constitutes a separate pore such as occurs with concatamers of two different ClC family members (Weinreich & Jentsch, 2001). However, in that case, in contrast to the situation with CFTR, there is good biochemical and genetic evidence that these are dimeric

proteins (Steinmeyer et al., 1994; Jentsch et al., 1999).

Discussion

Knowledge of a protein's quaternary structure is essential to an understanding of its mechanism of action. Homo- or hetero-oligomeric structures are common, especially in prokaryotes where the mean length of individual polypeptides is relatively short compared with larger multi-domain proteins that are more common in eukaryotes (Doolittle, 1995). This paradigm is indeed well illustrated by ABC proteins where in many prokaryotic transporters each of the nucleotide-binding and membrane-integrated domains are products of separate polycistronic transcripts, whereas in eukaryotic versions these are fused into single or at most two mRNAs (Higgins, 1992). As mentioned in the Introduction, it is still less clear whether more than one four-domain unit is required for function. The only well-established examples of hetero-oligomeric structures involving ABC proteins are the K_{ATP} channels where a sulfonylurea receptor of the ABCC subfamily associates with an inwardly rectifying potassium channel subunit (Aguilar-Bryan et al., 1998). Since these latter subunits form homotetramers as in other potassium channels, K_{ATP} channels are octameric (Clement et al., 1997; Inagaki et al., 1997; Shyng & Nichols, 1997).

Other potassium channels that are either voltage or ligand gated have similar homo-tetrameric pores (MacKinnon, 1991, 1995; Yang et al., 1995; Doyle et al., 1998). Other cation channels involved in membrane excitability, such as sodium and calcium channels, have repeat units in longer single polypeptides rather than separate pore-forming subunits that assemble (Catterall, 1988). However, while these large repeat-containing α subunits are usually capable of basic channel activity, they often associate with smaller regulatory subunits (Walker & De Waard, 1998; Catterall, 2000). The large family of ligand-gated channels typified by the nicotinic acetylcholine receptor are heteroligomeric (Cooper et al., 1991; Unger et al., 1999) as are in fact the majority of other known channels (Hille, 2001).

Interestingly, compared with the channels alluded to above that are cation channels, the major class of anion channels, members of the large ClC family (Jentsch et al., 1999; Maduke, Miller & Mindell, 2000), are double-barreled homodimers with each large polypeptide chain containing multiple membrane-spanning helices (Fahlke et al., 1997; Mindell et al., 2001; Weinreich & Jentsch, 2001; Dutzler et al., 2002). Consistent with their structures as homodimers, ClC mutations, including those causing several different diseases, are dominant (Koch et al., 1992; Steinmeyer et al., 1994).

Of the approximately 1000 disease-associated mutations identified in the CFTR gene, none exhibit dominant behaviors and hence there is no genetic evidence indicating that the CFTR chloride channel may be other than monomeric. It is of course possible that any potential dominant negative effect of one mutant subunit in a CFTR oligomer might be incomplete as only a small number of active molecules may be sufficient for physiological function (Johnson et al., 1992). The results we obtained with the co-expression of wild-type and ΔF508 CFTR corroborate the in vivo evidence that this mutant has no detectable dominant negative action. We have also directly tested whether more than one CFTR polypeptide contributes to the chloride ion pore by co-expressing forms with different amino acids at positions within TM6 known to strongly influence unitary conductance (Tabcharani et al., 1993; McDonough et al., 1994; Linsdell et al., 1997). Although the two forms were expressed in approximately equal amounts as judged by detection of different epitope tags attached to each, channels of conductances other than those of the two co-expressed were not detected at frequencies higher than when these species were expressed separately. Given the strong evidence that residues within TM6 contribute directly to pore formation (Dawson et al., 1999; Smith et al., 2001), TM6s from each form expressed should have influenced pore properties if two CFTR polypeptides are required for its formation.

Supportive of these electrophysiological findings were the observations that CFTR polypeptides were not found to be self-associated when solubilized under mild conditions from membranes of cells expressing the protein heterologously or endogenously. In both cases, the protein sedimented as a single uniform species of size approximating that of a monomer with bound detergent. No larger species representing either oligomers or non-specific aggregates were detected.

As an additional very sensitive means of detecting associations between individual CFTR polypeptides, they were distinctly tagged with different epitopes at either the N- or C-termini and co-expressed. Although each was readily immunoprecipitated with antibody to the epitope it contained, none of the form containing the other epitope was coprecipitated. Conditions that activate CFTR channels, such as forskolin treatment of cells, did not alter these distributions. While it might be argued that such a result might be expected with the PDZ-domain-binding C-termini blocked by the fused epitopes or absent in the case of the similar experiments of Marshall et al. (1994), the N-terminally tagged forms would not be compromised in this way. Even overexpression of EBP-50 did not lead to any detectible associations. This would indicate that if the stimulatory effects of increasing amounts of EBP-50

(Raghuram et al., 2001) or CAP-70 (Wang et al., 2000) are due to mediated crosslinking of two CFTRs via their C-termini, the proportion of the bulk CFTR population so affected must be very small. This would of course not mean that it is functionally unimportant.

To conclude, it may be worth considering the difference between the possibility of the CFTR channel possessing a true quaternary structure, in which contributions from more than one CFTR polypeptide chain are essential to pore formation and the tethering together of two or more chains, which might modulate the activity of either. Neither our present study nor any of those previously published (Zerhusen et al., 1999; Wang et al., 2000; Raghuram et al., 2001; Ramjeesingh et al., 2001) provides any evidence that a higher structure than a monomer is essential for channel function. Zerhusen et al. (1999) showed that a forced dimer had somewhat different properties from the native state, i.e., with low-level heterologous expression of a non-concatamerized construct or endogenous expression. These investigators did not show that a monomeric species was inactive. Similarly the studies of Wang et al. (2000) and Raghuram et al. (2001) showed only that bivalent PDZ-domain protein addition modulated CFTR-channel activity. The latter authors interpreted this as evidence of a stable dimer, whereas the former group acknowledged alternative explanations. The more recent report of Ramjeesingh et al. (2001) unequivocally states that a CFTR monomer is sufficient for both channel and ATPase activity, although larger dimeric species were also detected. In agreement with these observations we have found in extensive chemical crosslinking studies (Chen and Riordan, *unpublished data*) that heterologously overexpressed CFTR can be crosslinked to large molecular complexes containing more than one CFTR species and other proteins.

Final proof of CFTR quaternary structure awaits determination of the 3-dimensional structure of the active purified protein. The two mammalian ABC proteins for which low-resolution 3-D structures have been determined have yielded two different results. P-glycoprotein appears monomeric in 2-dimensional crystals (Rosenberg et al., 1997), while multidrug resistance protein 1 appears dimeric (Rosenberg et al., 2001). Interestingly, the diameters of P-gp freeze-fracture particles in the membrane (~10 nm; Sehested et al., 1989; Arsenault, Ling & Kartner, 1988), and of 2-D crystalline arrays of the purified protein (10–12 nm; Rosenberg et al., 1997) are very similar. Furthermore, although interpreted by the authors as dimeric, the CFTR freeze-fracture particles in *Xenopus* oocyte membranes had virtually identical dimensions (~9 nm; Eskandari et al., 1998). The MsbA lipid A transporter of *E. coli* (Chang & Roth, 2001) when crystallized consists of two fused nucleotide-binding and membrane-integrated polypeptides or is monomeric in the terminology of the single-chain eukaryotic family members such as CFTR as is the BtuCD vitamin B12 importer (Locher et al. 2000).

This work was supported by the NIDDK of the NIH (DK51619) and the Cystic Fibrosis Foundation. J.-H. C. is a recipient of the Howard B. Burchell Scholarship from the American Heart Association. We thank Dr. Joseph Bryan for technical advice concerning velocity gradient centrifugation, and Sharon Fleck and Marv Ruona for assistance with preparation of the manuscript and the figures, respectively.

References

Aguilar-Bryan, L., Clement, J.P., Gonzalez, G., Kunjilwar, K., Babenko, A., Bryan, J. 1998. Toward understanding the assembly and structure of KATP channels, *Physiol. Rev.* **78:**227–245

Aleksandrov, A.A., Riordan, J.R. 1998. Regulation of CFTR ion channel gating by MgATP. *FEBS Lett.* **431:**97–101

Arsenault, A.L., Ling, V., Kartner, N. 1988. Altered plasma membrane ultrastructure in multidrug-resistant cells. *Biochim. Biophys. Acta* **938:**315–321

Bear, C.E., Li, C.H., Kartner, N., Bridges, R.J., Jensen, T.J., Ramjeesingh, M, Riordan, J.R. 1992. Purification and functional reconstitution of the cystic fibrosis transmembrane conductance regulator (CFTR). *Cell* **68:**809–818

Boscoboinik, D., Debanne, M.T., Stafford, A.R., Jung, C.Y., Gupta, R.S., Epand, R.M. 1990. Dimerization of the P-glycoprotein in membranes. *Biochim. Biophys. Acta* **1027:**225–228

Catterall, W.A. 1988. Structure and function of voltage-sensitive ion channels. *Science* **242:**50–61

Catterall, W.A. 2000. From ionic currents to molecular mechanisms: the structure and function of voltage-gated sodium channels. *Neuron* **26:**13–25

Chan, K.W., Csanady, L., Seto-Young, D., Nairn, A.C., Gadsby, D.C. 2000. Severed molecules functionally define the boundaries of the cystic fibrosis transmembrane conductance regulator's NH(2)-terminal nucleotide binding domain. *J. Gen. Physiol.* **116:**163-180

Chang, X.B., Hou, Y.X., Jensen, T.J., Riordan, J.R. 1994. Mapping of cystic fibrosis transmembrane conductance regulator membrane topology by glycosylation site insertion. *J Biol. Chem.* **269:**18572-5

Chang, G., Roth, C.B. 2001. Structure of MsbA from *E. coli*: a homolog of the multidrug resistance ATP binding cassette (ABC) transporters. *Science* **293:**1793–1800

Chang, G., Spencer, R.H., Lee, A.T., Barclay, M.T., Rees, B.C. 1998. Structure of the MscL homolog from Mycobacterium tuberculosis: a gated mechanosensitive ion channel. *Science* **282:**2220–2226

Cheng, S.H., Gregory, R.J., Marshall, J., Paul, S., Souza, D.W., White, G.A., O'Riordan, C.R., Smith, A.E. 1990. Defective intracellular transport and processing of CFTR is the molecular basis of most cystic fibrosis. *Cell* **63:**827-34

Clement, J.P.t., Kunjilwar, K., Gonzalez, G., Schwanstecher, M., Panten, U., Aguilar-Bryan, L., Bryan, J. 1997. Association and stoichiometry of K(ATP) channel subunits. *Neuron* **18:**827–838

Cooper, E., Couturier, S., Ballivet, M. 1991. Pentameric structure and subunit stoichiometry of a neuronal nicotinic acetylcholine receptor. *Nature* **350:**235–238

Corey, S., Krapivinsky, G., Krapivinsky, L., Clapham, D.E. 1998. Number and stoichiometry of subunits in the native atrial G-protein-gated K^+ channel, IKACh. *J. Biol. Chem.* **273:**5271–5278

Dawson, D.C., Smith, S.S., Mansoura, M.K. 1999. CFTR: mechanism of anion conduction. *Physiol. Rev.* **79:**S47–S75

Dean, M., Rzhetsky, A., Allikmets, R. 2001. The human ATP-binding cassette (ABC) transporter superfamily. *Genome Res.* **11:**1156–1166

Doige, C.A., Ames, G.F. 1993. ATP-dependent transport systems in bacteria and humans: relevance to cystic fibrosis and multidrug resistance. *Annu. Rev. Microbiol.* **47:**291–319

Doolittle, R.F. 1995. The multiplicity of domains in proteins. *Annu. Rev. Biochem.* **64:**287–314

Doyle, D.A., Morais Cabral, J., Pfuetzner, R.A., Kuo, A., Gulbis, J.M., Cohen, S.L., Chait, B.T., MacKinnon, R. 1998. The structure of the potassium channel: molecular basis of K^+ conduction and selectivity. *Science* **280:**69–77

Dutzler, R., Campbell, E.B., Cadene, M., Chait, B.T., MacKinnon, R. 2002. X-ray structure of a CIC chloride channel at 3.0 A reveals the molecular basis of anion selectivity. *Nature* **415:**287-94

Eskandari, S., Wright, E.M., Kreman, M., Starace, D.M., Zampighi, G.A. 1998. Structural analysis of cloned plasma membrane proteins by freeze-fracture electron microscopy. *Proc. Natl. Acad. Sci. USA* **95:**11235–11240

Fahlke, C., Knittle, T., Gurnett, C.A., Campbell, K.P., George Jr., A.L., 1997. Subunit stoichiometry of human muscle chloride channels. *J. Gen. Physiol.* **109:**93–104

Fanning, A.S., Anderson, J.M. 1999. PDZ domains: fundamental building blocks in the organization of protein complexes at the plasma membrane. *J. Clin. Invest.* **103:**767–772

Garner, C.C., Nash, J., Huganir, R.L. 2000. PDZ domains in synapse assembly and signalling. *Trends Cell Biol.* **10:**274–280

Gregory, R.J., Cheng, S.H., Rich, D.P., Marshall, J., Paul, S., Hehir, K., Ostedgaard, L., Klinger, K.W., Welsh, M.J., Smith, A.E. 1990. Expression and characterization of the cystic fibrosis transmembrane conductance regulator. *Nature* **347:**382-6

Gunderson, K.L., Kopito, R.R. 1995. Conformational states of CFTR associated with channel gating: the role ATP binding and hydrolysis. *Cell* **82:**231–239

Hall, R.A., Ostedgaard, L.S., Premont, R.T., Blitzer, J.T., Rahman, N., Welsh, M.J., Lefkowitz, R.J. 1998. A C-terminal motif found in the beta2-adrenergic receptor, P2Y1 receptor and cystic fibrosis transmembrane conductance regulator determines binding to the Na^+H^+ exchanger regulatory factor family of PDZ proteins. *Proc. Natl. Acad. Sci. USA* **95:**8496–8501

Hämmerle, M.M., Aleksandrov, A.A., Chang, X., Riordan, J.R. 2000. A novel CFTR disease-associated mutation causes addition of an extra N-linked oligosaccharide. *Glycoconj J* **17:** 807-13

Haws, C., Finkbeiner, W.E., Widdicombe, J.H., Wine, JJ. 1994. CFTR in Calu-3 human airway cells: channel properties and role in cAMP-activated Cl-conductance. *Am. J. Physiol.* **266:**L502–L512

Higgins, C.F. 1992. ABC transporters: from microorganisms to man. *Annu. Rev. Cell Biol.* **8:**67–113

Hille, B. 2001. Ion channels of excitable membranes. Sinauer, Sunderland, Mass.

Hurtley, S.M., Helenius, A. 1989. Protein oligomerization in the endoplasmic reticulum. *Annu. Rev. Cell. Biol.* **5:**227–307

Inagaki, N., Gonoi, T., Seino, S. 1997. Subunit stoichiometry of the pancreatic beta-cell ATP-sensitive K^+ channel. *FEBS Lett.* **409:**232–236

Jensen, T.J., Loo, M.A., Pind, S., Williams, D.B., Goldberg, A.L., Riordan, J.R. 1995. Multiple proteolytic systems, including the proteasome, contribute to CFTR processing. *Cell* **83:**129–135

Jentsch, T.J., Friedrich, T., Schriever, A., Yamada, H. 1999. The CLC chloride channel family. *Pfluegers Arch.* **437:**783–795

Jette, L., Potier, M., Beliveau, R. 1997. P-glycoprotein is a dimer in the kidney and brain capillary membranes: effect of cyclosporin A and SDZ-PSC 833. *Biochemistry* **36:**13929–13937

Johnson, L.G., Olsen, J.C., Sarkadi, B., Moore, K.L., Swanstrom, R., Boucher, R.C. 1992. Efficiency of gene transfer for restoration of normal airway epithelial function in cystic fibrosis. *Nat. Genet.* **2:**21–25

Juvvadi, S.R., Glavy, J.S., Horwitz, S.B., Orr, G.A. 1997. Domain organization of murine mdrlb P-glycoprotein: the cytoplasmic linker region is a potential dimerization domain. *Biochem. Biophys. Res. Comm.* **230:**442–447

Kartner, N., Riordan, J.R. 1998. Characterization of polyclonal and monoclonal antibodies to cystic fibrosis transmembrane conductance regulator. *Methods Enzymol.* **292:**629–652

Koch, M.C., Steinmeyer, K., Lorenz, C., Ricker, K., Wolf, F., Otto, M., Zoll, B., Lehmann-Horn, F., Grzeschik, K.H., Jentsch, TJ. 1992. The skeletal muscle chloride channel in dominant and recessive human myotonia. *Science* **257:**797–800

Kocher, O., Cornelia, N., Gilchrist, A., Pal, R., Tognazzi, K., Brown, L.F., Knoll, J.H. 1999. PDZK1, a novel PDZ domain-containing protein up-regulated in carcinomas and mapped to chromosome Iq21, interacts with cMOAT (MRP2), the multidrug resistance-associated protein. *Lab. Invest.* **79:**1161–1170

Koronakis, V., Sharff, A., Koronakis, E., Luisi, B., Hughes, C. 2000. Crystal structure of the bacterial membrane protein TolC central to multidrug efflux and protein export. *Nature* **405:**914–919

Liman, E.R., Tytgat, J., Hess, P. 1992. Subunit stoichiometry of a mammalian K^+ channel determined by construction of multimeric cDNAs. *Neuron* **9:**861–871

Linsdell, P., Tabcharani, J.A., Rommens, J.M., Hou, Y.X., Chang, X.B., Tsui, L.C., Riordan, J.R., Hanrahan, J.W. 1997. Permeability of wild-type and mutant cystic fibrosis transmembrane conductance regulator chloride channels to polyatomic anions. *J. Gen. Physiol.* **110:**355–364

Locher, K.P., Lee, A.T., Rees, D.C. 2002. The E. coli BtuCD structure: a framework for ABC transporter architecture and mechanism. *Science* **296:**1091-8

Loo, M.A., Jensen, T.J., Cui, L., Hou, Y., Chang, X.B., Riordan, J.R. 1998. Perturbation of Hsp90 interaction with nascent CFTR prevents its maturation and accelerates its degradation by the proteasome. *Embo J.* **17:**6879–6887

Loo, T.W., Clarke, D.M. 1996. The minimum functional unit of human P-glycoprotein appears to be a monomer. *J. Biol. Chem.* **271:**27488–27492

Lukacs, G.L., Mohamed, A., Kartner, N., Chang, X.B., Riordan, J.R., Grinstein, S. 1994. Conformational maturation of CFTR but not its mutant counterpart (delta F508) occurs in the endoplasmic reticulum and requires ATP. *Embo J.* **13:**6076–6086

MacKinnon, R. 1991. Determination of the subunit stoichiometry of a voltage-activated potassium channel. *Nature* **350:**232–235

MacKinnon, R. 1995. Pore loops: an emerging theme in ion channel structure. *Neuron* **14:**889–892

Maduke, M., Miller, C., Mindell, J.A. 2000. A decade of CLC chloride channels: structure, mechanism, and many unsettled questions. *Annu. Rev. Biophys. Biomol. Struct.* **29:**411–438

Marshall, J., Fang, S., Ostedgaard, L.S., O'Riordan, C.R., Ferrara, D., Amara, J.F., Hoppe, H.T., Scheule, R.K., Welsh, M.J., Smith, A.E., et al. 1994. Stoichiometry of recombinant cystic fibrosis transmembrane conductance regulator in epithelial cells and its functional reconstitution into cells in vitro. *J. Biol. Chem.* **269:**2987–2995

McDonough, S., Davidson, N., Lester, H.A., McCarty, N.A. 1994. Novel pore-lining residues in CFTR that govern permeation and open-channel block. *Neuron* **13:**623–634

Mindell, J.A., Maduke, M., Miller, C., Grigorieff, N. 2001. Projection structure of a ClC-type chloride channel at 6.5 A resolution. *Nature* **409:**219–223

Naito, M., Tsuruo, T. 1992. Functionally active homodimer of P-glycoprotein in multidrug-resistant tumor cells. *Biochem. Biophys. Res. Comm.* **185:**284–290

Pind, S., Riordan, J.R., Williams, D.B. 1994. Participation of the endoplasmic reticulum chaperone calnexin (p88, IP90) in the biogenesis of the cystic fibrosis transmembrane conductance regulator. *J. Biol. Chem.* **269:**12784–12788

Poruchynsky, M.S., Ling, V. 1994. Detection of oligomeric and monomeric forms of P-glycoprotein in multidrug resistant cells. *Biochemistry* **33:**4163–4174

Raghuram, V., Mak, D.D., Foskett, J.K. 2001. Regulation of cystic fibrosis transmembrane conductance regulator single-channel gating by bivalent PDZ-domain-mediated interaction. *Proc. Natl. Acad. Sci. USA* **98:**1300–1305

Ramjeesingh, M., Li, C., Garami, E., Huan, L.J., Hewryk, M., Wang, Y., Galley, K., Bear, C.E. 1997. A novel procedure for the efficient purification of the cystic fibrosis transmembrane conductance regulator (CFTR). *Biochem. J.* **327:**17–21

Ramjeesingh, M., Li, C., Kogan, L, Wang, Y., Huan, L.J., Bear, C.E. 2001. A monomer is the minimum functional unit required for channel and ATP activity of the cystic fibrosis transmembrane conductance regulator. *Biochemistry* **40:**10700–10706

Rosenberg, M.R, Callaghan, R., Ford, R.C., Higgins, C.F. 1997. Structure of the multidrug resistance P-glycoprotein to 2.5 nm resolution determined by electron microscopy and image analysis. *J. Biol. Chem.* **272:**10685–10694

Rosenberg, M.F., Mao, Q., Holzenburg, A., Ford, R.C., Deeley, R.G., Cole, S.P. 2001. The structure of the multidrug resistance protein 1 (MRP1/ABCC1). Crystallization and single-particle analysis. *J. Biol. Chem.* **276:**16076–16082

Sambrook, J., Russell, D.W. 2001. Molecular cloning: a laboratory manual. Cold Spring Harbor Laboratory Press, Cold Spring Harbor, NY

Sato, S., Ward, C.L., Kopito, R.R. 1998. Cotranslational ubiquitination of cystic fibrosis transmembrane conductance regulator in vitro. *J. Biol. Chem.* **273:**7189–7192

Schillers, H., Danker, T., Madeja, M., Oberleithner, H. 2001. Plasma membrane protein clusters appear in CFTR-expressing *Xenopus laevis* oocytes after cAMP stimulation. *J. Membrane Biol.* **180:**205–212

Sehested, M., Simpson, D., Skovsgaard, T., Buhl-Jensen, P. 1989. Freeze-fracture study of plasma membranes in wild type and daunorubicin-resistant Ehrlich ascites tumor and P388 leukemia cells. *Virchows Arch. B Cell Pathol. Incl. Mol. Pathol.* **56:**327–335

Shen, B.Q., Finkbeiner, W.E., Wine, J.J., Mrsny, R.J., Widdicombe, J.H. 1994. Calu-3: a human airway epithelial cell line that shows cAMP-dependent Cl-secretion. *Am. J. Physiol.* **266:**L493–L501

Sheng, M., Sala, C. 2001. PDZ domains and the organization of supramolecular complexes. *Annu. Rev. Neurosci.* **24:**1–29

Short, D.B., Trotter, K.W., Reczek, D., Kreda, S.M., Bretscher, A., Boucher, R.C., Stutts, M.J., Milgram, S.L. 1998. An apical PDZ protein anchors the cystic fibrosis transmembrane conductance regulator to the cytoskeleton. *J. Biol. Chem.* **273:**19797–19801

Shyng, S., Nichols, C.G. 1997. Octameric stoichiometry of the KATP channel complex. *J. Gen. Physiol.* **110:**655–664

Smith, S.S., Liu, X., Zhang, Z.R., Sun, F., Kriewall, T.E., McCarty, N.A., Dawson, B.C. 2001. CFTR. Covalent and noncovalent modification suggests a role for fixed charges in anion conduction. *J. Gen. Physiol.* **118:**407–432

Song, L., Hobaugh, M.R., Shustak, C., Cheley, S., Bayley, H., Gouaux, J.E. 1996. Structure of staphylococcal alpha-hemolysin, a heptameric transmembrane pore. *Science* **274:**1859–1866

Steinmeyer, K., Lorenz, C., Pusch, M., Koch, M.C., Jentsch, T.J. 1994. Multimeric structure of ClC-1 chloride channel revealed by mutations in dominant myotonia congenita (Thomsen). *Embo J.* **13:**737–743

Sun, F., Hug, M.J., Lewarchik, C.M., Yun, C., Bradbury, N.A., Frizzell, R.A. 2000. E3KARP mediates the association of ezrin and protein kinase A with the cystic fibrosis transmembrane conductance regulator in airway cells. *J. Biol. Chem.* **275:**29539–29546

Tabcharani, J.A., Rommens, J.M., Hou, Y.X., Chang, X.B., Tsui, L.C., Riordan, J.R., Hanrahan, J.W. 1993. Multi-ion pore behaviour in the CFTR chloride channel. *Nature* **366:**79–82

Taylor, J.C., Horvath, A.R., Higgins, C.F., Begley, G.S. 2001. The multidrug resistance p-glycoprotein oligomeric state and intramolecular interactions. *J. Biol. Chem.* **276:**36075–36078

Unger, V.M., Kumar, N.M., Gilula, N.B., Yeager, M. 1999. Three-dimensional structure of a recombinant gap junction membrane channel. *Science* **283:**1176–1180

von Heijne, G. 1997. Membrane protein assembly. Chapman & Hall, New York

Walker, D., De Waard, M. 1998. Subunit interaction sites in voltage-dependent Ca^{2+}-channels: role in channel function. *Trends Neurosci.* **21:**148–154

Wang, S., Raab, R.W., Schatz, P.J., Guggino, W.B., Li, M. 1998. Peptide binding consensus of the NHE-RF-PDZ1 domain matches the C-terminal sequence of cystic fibrosis transmembrane conductance regulator (CFTR). *FEBS Lett.* **427:**103–108

Wang, S., Yue, H., Derin, R.B., Guggino, W.B., Li, M. 2000. Accessory protein facilitated CFTR-CFTR interaction, a molecular mechanism to potentiate the chloride channel activity. *Cell* **103:**169–179

Ward, C.L., Omura, S., Kopito, R.R. 1995. Degradation of CFTR by the ubiquitin-proteasome pathway. *Cell* **83:**121–127

Weinreich, F., Jentsch, T.J. 2001. Pores formed by single subunits in mixed dimers of different CLC chloride channels. *J. Biol. Chem.* **276:**2347–2553

Yang, J., Jan, Y.N., Jan, L.Y. 1995. Determination of the subunit stoichiometry of an inwardly rectifying potassium channel. *Neuron* **15:**1441–1447

Zerhusen, B., Zhao, J., Xie, J., Davis, P.B., Ma, J. 1999. A single conductance pore for chloride ions formed by two cystic fibrosis transmembrane conductance regulator molecules. *J. Biol. Chem.* **274:**7627–7630